



Contribution of multiple reflections to light utilization efficiency of submicron hollow TiO₂ photocatalyst

Hongyan Liu^{1,2,3*}, Hua Ma², Jibong Joo^{2,4} and Yadong Yin^{2*}

ABSTRACT In this work, we carried out both theoretical calculation and experimental studies to reveal the contribution of hollow geometry to the light utilization efficiency of the TiO₂ photocatalysts in diluted aqueous solution. It is found that the single or multi-shelled hollow structures do not induce significant multiple reflections within the shells as widely believed in previous reports, and therefore the geometric factor has minimal contribution to the improvement of the light utilization efficiency of the photocatalyst. To design TiO₂ photocatalysts with higher activity, it is more appropriate to focus on the improvement of the crystallinity, diffusion, surface area, and dispersity of the catalysts, rather than their geometric shapes.

Keywords: multiple reflections, photocatalysis, TiO₂, hollow shell

INTRODUCTION

Hollow structures of inorganic materials have attracted much attention because of their widespread potential applications in catalysis, controlled delivery, photonic devices, biomedicine, and energy [1–7]. For applications in environmental and energy-related systems, various hollow spheres of metal, metal oxide, and carbon-based materials have been used in dye-sensitized solar cells [8], photocatalysis [9], fuel cells [10], lithium ion batteries [11], and supercapacitors [12]. It has been proven that the unique structure of hollow spheres provides an enhanced surface-to-volume ratio and reduced transport lengths for both mass and charge transport [13]. Particular interests have been attracted to the synthesis of hollow structures of TiO₂, one of the most widely studied semiconducting oxide materials, and their applications in solar energy conversion

[14]. In addition to the intrinsic materials characteristics including low cost, low toxicity, and high chemical and optical stability [15,16], hollow nanostructures of TiO₂ are believed to be able to provide a high active surface area, reduced diffusion resistance, and improved accessibility, which are beneficial features for photocatalysis. We have previously synthesized mesoporous hollow TiO₂ shells with high surface areas through a surface-protected calcination process, revealed how the surface coating of another oxide or polymer could affect the crystallinity and the catalytic activity of the shells, and demonstrated that the phase composition, degree of crystallinity, surface area, and dispersity of TiO₂ were important features required for photocatalysis [17–20].

In solar energy conversion, one of the widely emphasized advantages of the TiO₂ hollow structures is the enhanced light utilization efficiency. For example, Li *et al.* [21] found that the photocatalytic activity of the “semi-hollow” core-shell structured TiO₂ increased compared to the “fully-hollow” structured TiO₂, suggesting that the multiple reflections of the incident light within the interior cavity of the hollow structure resulted in an enhanced light harvesting efficiency. This claim of enhancement of the photocatalytic activity by multiple reflections was echoed by others for TiO₂ hollow structures [22–25], and also claimed later for other hollow materials such as ZnO [26,27], NiO [28], SnO [29], CdS [30], Fe₂O₃ [31] and carbon nitride [32]. However, as generally known, the multiple reflections within the interior cavity should occur only when the cavity diameter is much larger than the wavelength of the incident light [33,34]. Since many of the previous claims were

¹ Key Laboratory of Luminescent and Real-Time Analytical Chemistry, Ministry of Education, College of Chemistry and Chemical Engineering, Southwest University, Chongqing 400715, China

² Department of Chemistry and UCR Center for Catalysis, University of California, Riverside, CA 92521, USA

³ College of Chemistry and Chemical Engineering, Lanzhou University, Lanzhou 730000, China

⁴ Department of Chemical Engineering, Konkuk University, 120 Neungdong-Ro, Gwangjin-Gu, Seoul, Republic of Korea

* Corresponding authors (emails: liuhy860@swu.edu.cn (Liu H); yadong.yin@ucr.edu (Yin Y))

made based on submicron hollow structures, it remained a question if hollow structures of this dimension can indeed induce multiple reflections and benefit the light utilization efficiency of the photocatalysts.

In this work, we carried out both theoretical calculation and experimental studies to reveal the contribution of hollow geometry to the light utilization efficiency of the TiO₂ photocatalyst. We show that the hollow or multi-shelled hollow structures do not help much in improving the light utilization efficiency of the materials for photocatalysis. Calculations based on Mie scattering theory and experimental comparison of the photocatalytic activity of the TiO₂ hollow shells with that of crushed ones reveal that multiple reflections of 365 nm UV light are not notable in submicron TiO₂ hollow shells. The photocatalytic performance of TiO₂ hollow structures may be enhanced by the Mie resonances when the diameters of the TiO₂ shells match with the wavelength of the incident light. However, the activity enhancement is found to be still minor compared with other parameters such as crystallinity, diffusion resistance, surface area, and solution dispersibility of the catalyst.

EXPERIMENTAL SECTION

Chemicals

Tetraethylorthosilicate (TEOS, 99%), poly(vinyl pyrrolidone) (PVP, $M_w \sim 40,000$), ammonium hydroxide (NH₃·H₂O, 28% by weight in water), were purchased from Sigma-Aldrich. Ethanol was obtained from Fisher. Tetrabutyl orthotitanate (TBOT, 99%) was purchased from Fluka. Absolute ethyl alcohol (200 proof) was purchased from Gold Shield Chemical. All chemicals were used as received without further purification. Deionized water was used throughout the experiments.

Synthesis

SiO₂@TiO₂

Colloidal silica templates were prepared through a modified Stöber method [35,36]. TEOS (0.86 mL) was mixed with deionized water (4.3 mL) and ethanol (23 mL) and an aqueous solution of ammonia (28%), the size of SiO₂ could be tuned by adjusting the concentration of ammonia. By adding 0.3, 0.45, 0.55, 0.62 and 1 mL of ammonia, the size of the SiO₂ particles is 90, 140, 200, 330 and 490 nm, respectively. After stirring for 4 h, the SiO₂ particles were separated by centrifugation, washed three times with ethanol, and then re-dispersed in 20 mL of ethanol. The above silica solution (5 mL) was dispersed in a mixture of ethanol (15

mL) and acetonitrile (7 mL). After adding ammonia aqueous solution (28%, 0.2 mL), TBOT (0.4 mL) in a mixture of ethanol (3 mL) and acetonitrile (1 mL) was injected into the mixture. After stirring for 3 h, the precipitate was isolated by centrifugation, washed with ethanol to give SiO₂@TiO₂ core-shell composites.

SiO₂@TiO₂@SiO₂

Above SiO₂@TiO₂ particles were dispersed in 20 mL of water, treated with PVP (0.2 g) overnight to allow for the adsorption of PVP onto the TiO₂ surface, separated from solution by centrifugation, and then re-dispersed in 23 mL ethanol. The solution of SiO₂@TiO₂ was sequentially mixed with water (4.3 mL), TEOS (0.8 mL) and aqueous ammonia (28%, 0.62 mL). After stirring for 4 h, the resulting SiO₂@TiO₂@SiO₂ particles were centrifuged, washed three times with ethanol and dried under vacuum.

Calcination and etching

To crystallize the amorphous TiO₂ shell, the samples were dried under vacuum and heated in air to 900°C at a rate of 2.5°C min⁻¹ then held for 2 h and cooled to room temperature. To obtain hollow shells by removal of the SiO₂ core and SiO₂ shell, the calcined sample (100 mg) was dispersed in an aqueous NaOH solution (20 mL, 0.5 mol L⁻¹), which was then stirred for 4 h at 90°C. The etched microspheres were centrifuged and washed several times with deionized water and ethanol and dried under vacuum to obtain the final hollow shells.

Void@TiO₂@Void@TiO₂

The above SiO₂@TiO₂@SiO₂ with 330 nm SiO₂ as core template was coated with another layer of TiO₂ and SiO₂, followed by calcination and etching, resulting in the TiO₂ double-shelled structure void@TiO₂@void@TiO₂, noted as D-T550. To fabricate TiO₂ double-shelled structure with larger inter-shell distance, the process of SiO₂ coating on SiO₂@TiO₂ was repeated, and then followed the same TiO₂ coating procedure. The product was noted as D-T670.

Characterization

The sample morphology was characterized using transmission electron microscopy (TEM) (Tecnai12). Samples were prepared by placing a drop of a diluted alcohol dispersion of the products on the surface of a copper grid. Crystal phases were determined by X-ray diffraction (XRD) analysis using a Bruker D8 advance diffractometer with Cu-Kα radiation ($\lambda = 1.5406 \text{ \AA}$). Nitrogen adsorption isotherms were obtained at 77 K using a nitrogen sorption instrument (Quantachrome NOVA 4200e). Brunauer-Emmert-Teller

(BET) calculations utilized the adsorption branch of the isotherm. The crushing treatments for silica hollow particles were carried out by grinding 20 mg sample in an agate mortar by hand for about 5 min.

Catalytic activity tests

The photocatalytic activity was evaluated by following the degradation of Rhodamine B (RhB) as a function of time. Before the photocatalytic test was initiated, the catalyst was first irradiated under UV light for 30 min to remove any residual organic contaminants. The catalyst (5 mg) was dispersed in an aqueous RhB solution (25 mL, 2×10^{-5} mol L⁻¹) in a 50 mL reactor cell and the solution was stirred in dark condition for 30 min to ensure adsorption of the dye. A 300 W Hg lamp with a 365 nm filter was used as the source of excitation (Xujiang XPA-7). The concentration of RhB was measured using a UV-vis spectrophotometer (HR2000CG-UV-NIR, Ocean Optics). The concentration of RhB in the reaction media was followed as a function of time by using the intensity of the 553 nm absorption peak in order to obtain the kinetic data.

RESULTS AND DISCUSSION

It has been widely proposed that the multiple reflections of light within TiO₂ hollow spheres can improve light harvesting and therefore enhance the photocatalytic activity, as shown in Fig. 1a. In photocatalysis, the activity of a catalyst is usually evaluated based on the same mass of the semiconducting materials. Therefore, to investigate the effect of multiple reflections, we need to compare the light absorption of a TiO₂ sphere and a hollow shell with the same mass. Absorption cross section is a measurement for the probability of an absorption process. More generally, cross section is used to quantify the probability of a certain light-particle interaction. Thus, we firstly calculated the cross sections of extinction, scattering, and absorption of solid and hollow TiO₂ spheres based on Mie scattering theory by assuming a fixed mass. As shown in Fig. 1b, the TiO₂ hollow shells evolve from a solid sphere by increasing the internal radius but maintaining the shell volume equal to the solid sphere. Firstly, TiO₂ hollow shells with the diameters ranged within 0–600 nm was calculated, as shown in Figs 1c–e. The scale bar from blue to red represents the

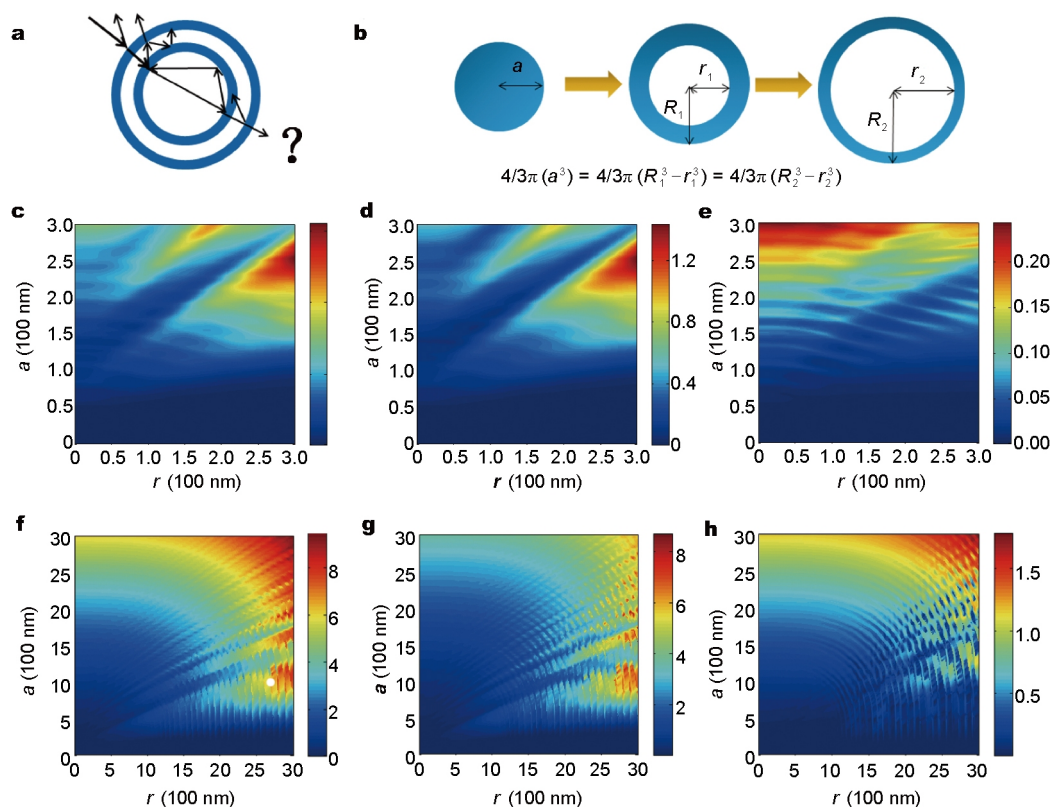


Figure 1 (a) The schematic of multiple reflections within the hollow structure (adapted from Ref. [23]). (b) The schematic evolution of a TiO₂ hollow shell from a solid sphere by gradually increasing the internal radius but maintaining the volume. Theoretical (c, f) extinction, (d, g) scattering and (e, h) absorption cross sections of the TiO₂ hollow shells to 365 nm UV light.

relative light intensity of the cross sections. In the simulations presented, the vertical axis indicates the radius of the solid TiO₂ spheres, while the horizontal axis indicates the internal radius of TiO₂ hollow shells. From this, it is observed that the extinction and the scattering intensity are very low in the Rayleigh region [33]; whereas in the Mie region, both the extinction and the scattering increase with the increasing of the solid particle size and the internal radius of hollow shells, showing a fluctuating distribution along the vertical and the horizontal axis. As a result, both the extinction and the scattering of hollow shell are much stronger than that of the corresponding solid sphere. The absorption also increases with the size of the TiO₂ spheres. Based on the same mass of TiO₂, with an increase of the radius of the inner cavity along the *x*-axis, the hollow shells become thinner and bigger. It is observed that the extinction of hollow shells is much stronger than the corresponding solid sphere (Fig. 1c). However, it can be found that the scattering of the hollow shell is also stronger than the solid one. By comparing the extinction and scattering, we are able to confirm that the higher extinction intensity of hollow shells is due to the scattering, rather than the absorption. The absorption of the hollow shell actually shows a similar intensity with the solid sphere (Fig. 1e), suggesting that there might be no multiple reflections within the hollow shell which can enhance the light harvesting efficiency. According to the theory of geometrical optics, the multiple reflections within the interior cavity of the hollow shell may occur when the particle size is much larger than the wavelength of the incident light [33,34]. Hence, we further expand the diameter of the TiO₂ shells up to 6 μm for calculation, with the simulated results shown in Figs 1f–h. The extinction and absorption of TiO₂ increase with the radius of solid spheres (*y* axis) and the internal radius of the hollow shells (*x* axis). By comparing the intensity of extinction, scattering, and absorption, it is found that for the larger TiO₂ particles, the extinction of light is mainly due to the absorption and the scattering is relatively low. The TiO₂ hollow shells show a notably stronger absorption than the solid sphere when the radius is beyond 1.5 μm (Fig. 1h), which can be explained by the possible multiple reflections within the cavity of the hollow structure. It seems reasonable then to conclude that for the submicron TiO₂ hollow shells, no multiple reflections would occur within the shells. Nonetheless, if the diameter of TiO₂ hollow shells is much larger (under geometrical optics approximation) than the wavelength of the incident light, there might be multiple reflections within the cavity of TiO₂ hollow shells and thus enhance the light harvesting efficiency.

Practically, it is difficult to synthesize a solid TiO₂ sphere and TiO₂ hollow shell with exactly the same mass and crystallinity to compare their photocatalytic activity. However, the activity enhancement of TiO₂ hollow spheres originating from the multiple reflections or the multiple scattering can be tested by comparing the activity before and after breaking the shells. It is assumed that the multiple reflections and the multiple scattering effects that happen on the TiO₂ hollow spheres are related to the diameter and shell thickness. Herein, the TiO₂ hollow structures with different diameters but similar thickness have been selectively fabricated. A series of hollow TiO₂ shells with particle diameters of 180–700 nm spanning over the UV and visible light regime was synthesized by using a SiO₂ templating method (see Supplementary information). The external diameters of the TiO₂ hollow spheres were controlled to be 190, 300, 450, and 600 nm (denoted as T190, T300, T450, and T600) by adopting 90, 200, 330, and 490 nm sized SiO₂ spheres as templates, respectively. TEM images of the hollow TiO₂ are shown in Figs 2a1–d1. The hollow TiO₂ samples show mesoporous structure with monodisperse particle dimensions (Fig. S1). Both the particle size and shell thickness are well controlled, showing a similar shell thickness of 50–60 nm. XRD was employed to further determine the crystalline phase of all TiO₂ hollow shells. As shown in Fig. S2, all samples show similar crystallinity with peaks attributable to the anatase crystalline phase of TiO₂.

For comparison, the hollow structure was destroyed by grinding of TiO₂ samples with an agate mortar, and then the photocatalytic activity of the resultant crushed sample was evaluated. As shown in Fig. S3, the hollow structure was totally destroyed after grinding. Sample T300 was chosen to investigate the change of BET surface area before and after grinding. As shown in Fig. S4, the BET surface area of T300 and the ground sample were 209 and 195 m² g⁻¹, respectively, suggesting no major change in the surface area. Afterwards, we tested the UV-driven degradation of RhB by using these samples as catalysts for evaluating the photocatalytic activity. The performance of photocatalysts toward RhB degradation was measured by monitoring the intensity changes of the 553 nm peak *versus* time, as summarized in Figs 2a2–d2. To compare the activity of TiO₂ hollow shells before (T) and after grinding (G), the data was also displayed in semilogarithmic form (inset in Figs 2a2–d2) in order to calculate the first-order reaction rate constants (*k*). For T190, the crushed sample shows a higher *k* value (0.039 min⁻¹) than the hollow shells (0.033 min⁻¹). The *k* value of T300, T450, and T600 are 0.029, 0.043, and 0.026 min⁻¹, respectively, while the crushed samples are

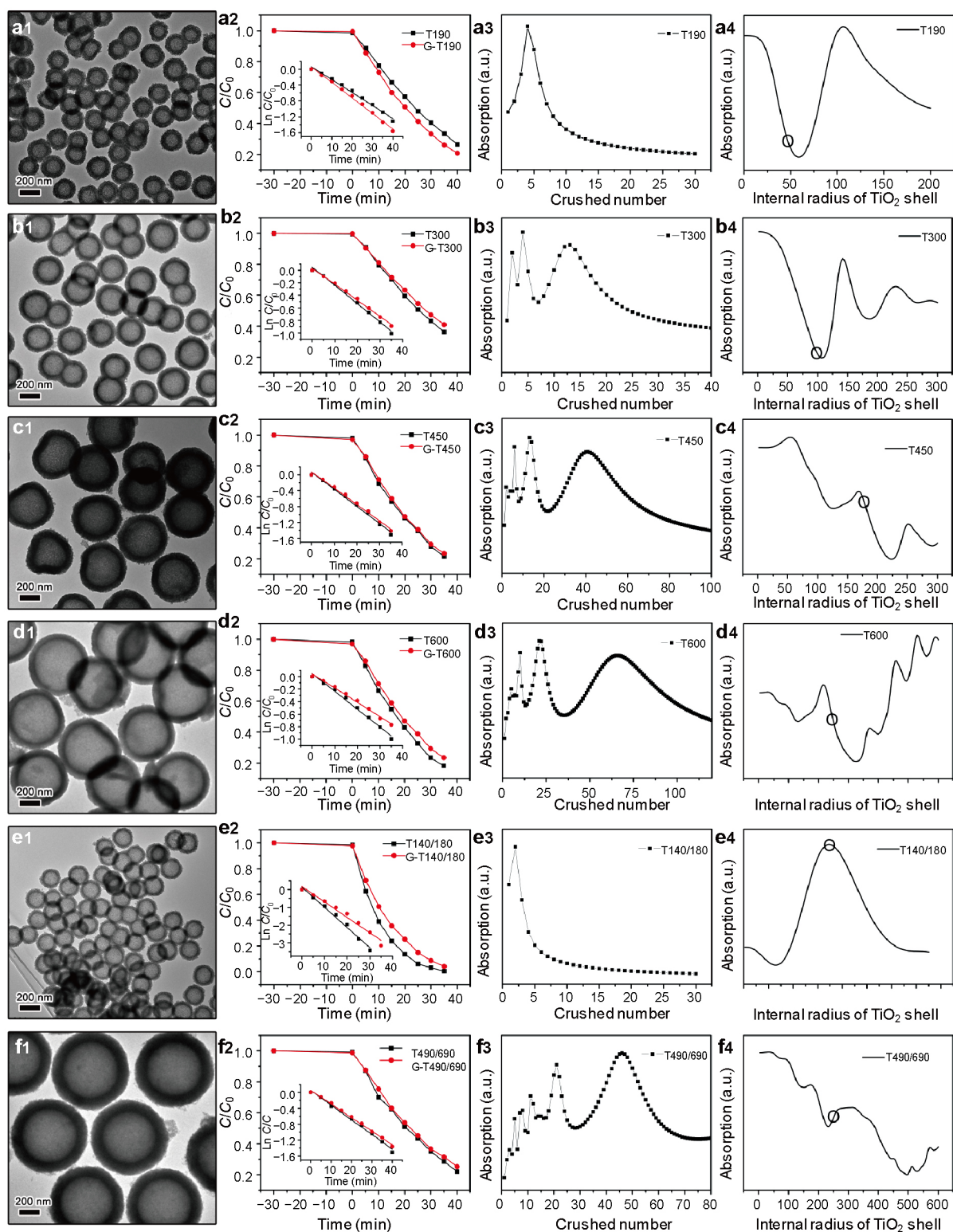


Figure 2 (a1–f1) TEM images of TiO₂ hollow shells, (a2–f2) the kinetic plots of the sample for photocatalytic degradation of RhB, and (a3–f3) the absorption cross section of the TiO₂ hollow shell over grinding; (a4–f4) the absorption cross section of a solid TiO₂ sphere evolved to hollow shells, and the circle indicates the position of the synthesized T190, T300, T450, T600, T140/180, and T490/690.

0.026, 0.041, and 0.027 min^{-1} , respectively. It is found that the activity differences of the sample before and after grinding are within 3%–10%, suggesting that there is no major light harvesting enhancement in the TiO_2 hollow shell.

In addition, we calculated the total absorption cross section of a TiO_2 hollow shell when cracked into several fragments, which is based on Scheme S1 and Equations (S5 and S6) (see Supplementary information). The simulation results show the absorption cross section of UV light (365 nm) *versus* crushing number (Figs 2a3–d3), which represents the number of the smaller pieces after crushing. Since it is hard to control how many small pieces are created after grinding, the trend of the absorption cross section *versus* crushing numbers can help us to understand the trend of activity changes. For the sample T190, as shown in Fig. 2a3, at the beginning of grinding, the absorption increases with the increase of crushed number, suggesting that the absorption can be enhanced by grinding. This can explain why the photocatalytic activity of T190 increases after grinding compared to the hollow shell structure. For T300, T450, and T600, at the beginning of crushing, the absorption is similar with that of the original TiO_2 hollow shell, showing a fluctuating trend. This is probably because of the different size distribution of the crushed samples. For the bigger and thicker hollow shells (T300, T450, and T600), the size distribution of the crushed fragments is broader than that of T190, so the ratio of the crushed fragments which show an appropriate size to cause the Mie resonance is higher, resulting in more absorption peaks, as shown in Figs 2b3–d3. The overall trend show a similar absorption, in accordance with the similar photocatalytic activity of these samples before and after grinding. Figs 2a4–d4 show the absorption cross section of each hollow shell evolution from a solid sphere with the mass equal to the hollow shell. The circles indicate the position of the synthesized TiO_2 hollow shell in this study. It is found that the hollow shell exhibits lower absorption compared to the solid particles. These results indicate that there is no multiple reflections in TiO_2 hollow shells from 190–600 nm with a thickness of about 50–60 nm.

To further evaluate the light utilization efficiency in TiO_2 hollow structures, we synthesized TiO_2 hollow shells with different shell thicknesses in order to investigate the light absorption as well as photocatalytic activity. Firstly, the external diameters of the TiO_2 hollow spheres were kept similar with T190 but the shell thickness was decreased by adopting 140 nm sized SiO_2 as the template, denoted as T140/180. As shown in Fig. 2e1, the hollow TiO_2 samples also show a mesoporous structure with a shell thickness of

about 20 nm. The photocatalytic activity of T140/180 before and after grinding was shown in Fig. 2e2. The crushed sample showed a lower activity ($k = 0.080 \text{ min}^{-1}$) compared to the hollow shells (0.096 min^{-1}). It is interesting that from the calculation result, it can be observed that the absorption cross section is decreasing over the grinding process (Fig. 2e3). The drop in activity may be attributed to the breakage of the hollow shells. According to Mie's scattering theory [34], the incident light will be strongly scattered on the surface of a particle with an appropriate size comparable to its wavelength. When the scattering cross-section exhibits a number of resonances for a given particle size, the scattering will be very efficient at these wavelengths. Here, the size of T140/180 likely matches the incident light (365 nm) to show Mie resonance, resulting in the enhancement of scattering and absorption of the TiO_2 hollow shell, followed by the high light utilization efficiency. It is also confirmed by the simulation of T140/180 from a solid sphere to a hollow shell by gradually increasing the internal radius but maintaining the volume. The calculated absorption was shown in Fig. 2e4. We can easily observe that a hollow shell with a 70 nm internal radius shows highest absorption intensity, which is consistent with the case of T140/180. After the hollow shells were destroyed, the resonant effect might be decreased or disappear, resulting in lower scattering and absorption and thus lower photocatalytic activity. Afterwards, a bigger and thicker TiO_2 hollow shell was prepared by increasing the thickness of T600, denoted as T490/690. As shown in Fig. 2f1, the hollow TiO_2 samples showed a shell thickness of about 100 nm. Similar photocatalytic activity was observed for T490/690 and the crushed sample (Fig. 2f2). The calculated absorption cross section also shows a fluctuating trend (Figs 2f3 and f4).

Recent works have also revealed that multi-shelled hollow spheres exhibit a greatly enhanced photocatalytic activity or photoelectric conversion efficiency due to multiple-reflections of light [37,38]. To verify the multiple reflections effect in the multi-shelled hollow TiO_2 , double shelled TiO_2 was synthesized by utilizing T450 (Fig. 3a1) as the inner hollow shell, sequential coating with SiO_2 and TiO_2 , and finally dissolving the middle layer of SiO_2 . Double shelled TiO_2 with different inter-shell distance were prepared, noted as D-T550 and D-T670, with their TEM images shown in Figs 3b1 and c1. It can be observed that the TiO_2 double shells have clear surfaces and a relatively darker core inside. Further investigation of a single sphere by high magnification TEM (inset of Figs 3b1 and c1) shows that the inter-shell distances of D-T550 and D-T670 are 10 and 75 nm, respectively. The photocatalytic activities of

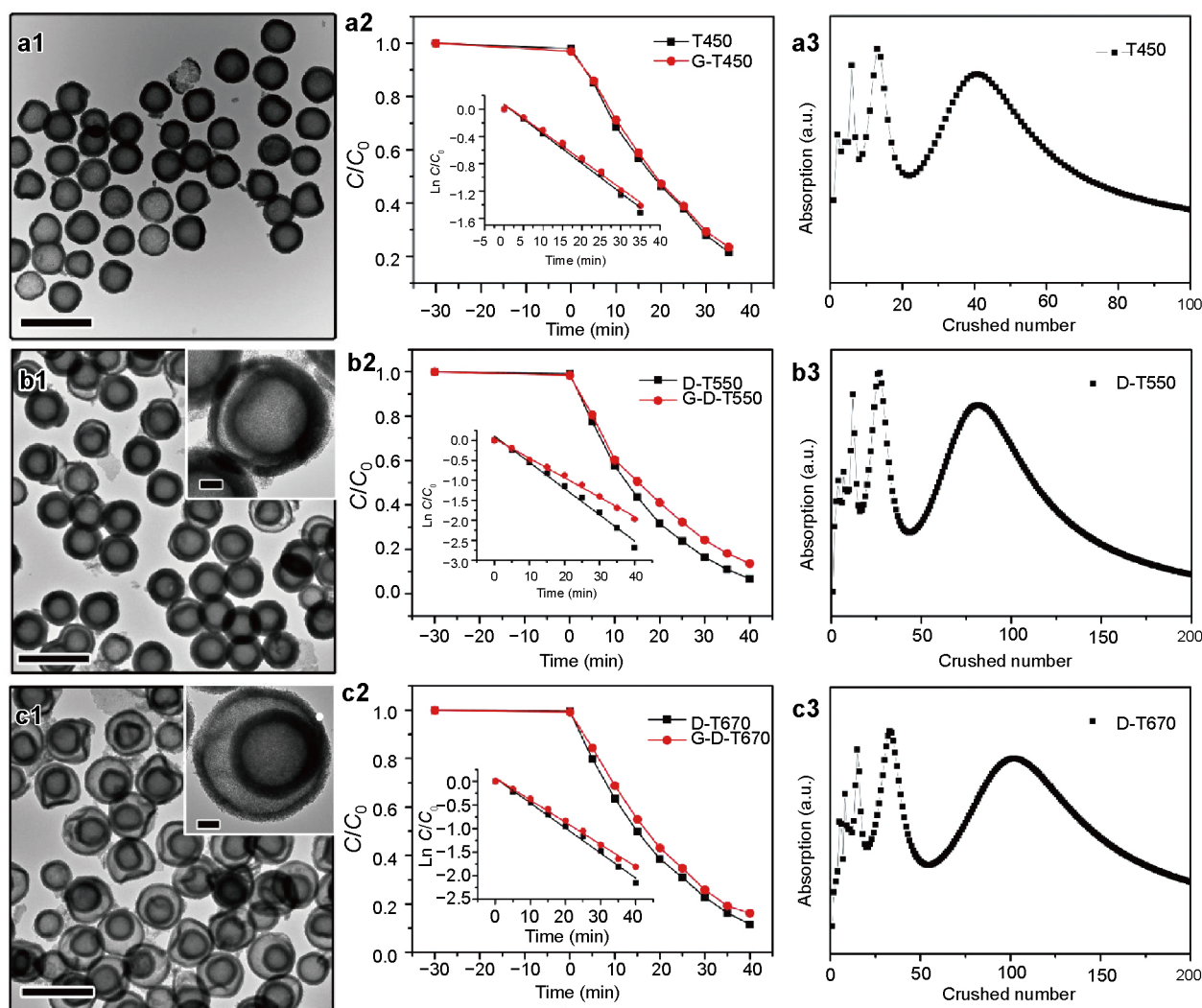


Figure 3 (a1, b1, c1) TEM images, (a2, b2, c2) the kinetic plots of the sample for photocatalytic degradation of RhB, and (a3, b3, c3) the absorption cross section of TiO_2 over grinding of T450, D-T550, D-T670. The scale bars in a1, b1, and c1 are 1 μm and 100 nm for the inset, respectively.

D-T550 and D-T-670 before and after grinding were evaluated by the degradation of RhB. The activity of sample D-T550 is shown in Fig. 3b2. It is found that the degradation activity of the double shell and crushed sample are almost the same within the first 10 min, after which the crushed sample shows a lower activity. The k value drops from 0.060 to 0.051 min^{-1} , which is probably due to the diffusion issue. As shown in Fig. 3c2, the crushed sample of D-T670 exhibits a very close degradation activity with the original TiO_2 double shell. The first-order reaction rate constants (k) calculated from the kinetic data (inset in Fig. 3c2) are 0.046 and 0.040 min^{-1} for D-T670 before and after grinding, respectively. There is not much difference in the observed activity, indicating that there are no significant multi-reflections of light within the double shell. The ab-

sorption cross section of D-T550 and D-T-670 over grinding was also calculated, as shown in Figs 3b3 and c3, where a fluctuating trend was observed for both of the two samples.

Finally, the photocatalytic activities of different TiO_2 hollow spheres before and after grinding are summarized in Fig. 4. On the basis of our experimental results, generally only a small difference in the activity was observed for the TiO_2 hollow shells before and after grinding. The activity differences are within the error range for most of the samples. A notable difference was for sample T140/180, as 17% decrease of the activity was observed after grinding. As we discussed previously, this is probably because of the match between the size of the shells (140/180 nm) and the incident light (365 nm), which leads to resonance and results in the

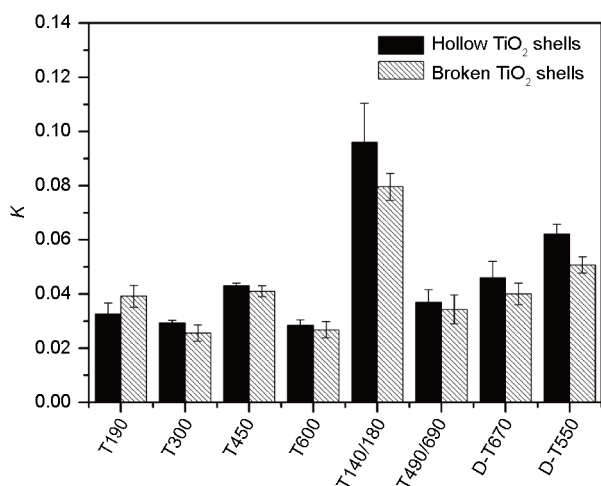


Figure 4 The comparison of the reaction kinetic constant values of different TiO₂ hollow shells before and after grinding.

highest light utilization efficiency and activity. However, compared with our previous results about the activity difference caused by the other factors such as crystallinity, phase composition, dispersity [20], the enhancement is more significantly, suggesting that the activity enhancement from the resonance is minor.

CONCLUSIONS

With theoretical and experimental evidences we reveal that the multiple reflections and multiple scattering of TiO₂ hollow structures are size dependent. In the submicron-scale TiO₂ hollow shells, there are no significant multiple reflections within the sphere interior voids. The photocatalytic performance of TiO₂ hollow structures can be enhanced by the Mie scattering of light only when the size of TiO₂ shell matches the wavelength of incident light. However, even when resonance is reached, the activity enhancement by scattering is still very limited. We conclude that for the design of TiO₂ photocatalyst with higher activity, it might be more appropriate to focus on the improvement of the crystallinity, diffusion, surface area, and dispersity of the catalyst, rather than its geometric shape. On the other hand, the fabrication processes of hollow shells do offer many other opportunities in structural design for achieving high active surface area, reduced diffusion resistance, and improved accessibility, which are highly desired features in photocatalysis.

Received 8 September 2016; accepted 22 September 2016;
published online 14 November 2016

- Caruso F, Caruso RA, Moehwald H. Nanoengineering of inorganic and hybrid hollow spheres by colloidal templating. *Science*, 1998,

- 282: 1111–1114
- 2 Arnal PM, Comotti M, Schüth F. High-temperature-stable catalysts by hollow sphere encapsulation. *Angew Chem*, 2006, 118: 8404–8407
- 3 He Q, Wu Z, Huang C. Hollow magnetic nanoparticles: synthesis and applications in biomedicine. *J Nanosci Nanotech*, 2012, 12: 2943–2954
- 4 Nai J, Tian Y, Guan X, *et al.* Pearson's principle inspired generalized strategy for the fabrication of metal hydroxide and oxide nanocages. *J Am Chem Soc*, 2013, 135: 16082–16091
- 5 Sun Y, Wiley B, Li ZY, *et al.* Synthesis and optical properties of nanorattles and multiple-walled nanoshells/nanotubes made of metal alloys. *J Am Chem Soc*, 2004, 126: 9399–9406
- 6 Fan C, Bian T, Shang L, *et al.* pH-Responsive reversible self-assembly of gold nanoparticles into nanovesicles. *Nanoscale*, 2016, 8: 3923–3925
- 7 Bian T, Shang L, Yu H, *et al.* Spontaneous organization of inorganic nanoparticles into nanovesicles triggered by UV light. *Adv Mater*, 2014, 26: 5613–5618
- 8 Koo HJ, Kim YJ, Lee YH, *et al.* Nano-embossed hollow spherical TiO₂ as bifunctional material for high-efficiency dye-sensitized solar cells. *Adv Mater*, 2008, 20: 195–199
- 9 Zhou C, Zhao Y, Bian T, *et al.* Bubble template synthesis of Sn₂Nb₂O₇ hollow spheres for enhanced visible-light-driven photocatalytic hydrogen production. *Chem Commun*, 2013, 49: 9872–9874
- 10 Liang HP, Zhang HM, Hu JS, *et al.* Pt hollow nanospheres: facile synthesis and enhanced electrocatalysts. *Angew Chem Int Ed*, 2004, 43: 1540–1543
- 11 Lou XW, Wang Y, Yuan C, *et al.* Template-free synthesis of SnO₂ hollow nanostructures with high lithium storage capacity. *Adv Mater*, 2006, 18: 2325–2329
- 12 Cao CY, Guo W, Cui ZM, *et al.* Microwave-assisted gas/liquid interfacial synthesis of flowerlike NiO hollow nanosphere precursors and their application as supercapacitor electrodes. *J Mater Chem*, 2011, 21: 3204–3209
- 13 Lai X, Halpert JE, Wang D. Recent advances in micro-/nano-structured hollow spheres for energy applications: from simple to complex systems. *Energy Environ Sci*, 2012, 5: 5604–5618
- 14 Zhao Y, Jia X, Waterhouse GIN, *et al.* Layered double hydroxide nanostructured photocatalysts for renewable energy production. *Adv Energy Mater*, 2016, 6: 1501974
- 15 Kudo A, Miseki Y. Heterogeneous photocatalyst materials for water splitting. *Chem Soc Rev*, 2009, 38: 253–278
- 16 Macwan DP, Dave PN, Chaturvedi S. A review on nano-TiO₂ sol-gel type syntheses and its applications. *J Mater Sci*, 2011, 46: 3669–3686
- 17 Joo JB, Zhang Q, Lee I, *et al.* Mesoporous anatase titania hollow nanostructures through silica-protected calcination. *Adv Funct Mater*, 2012, 22: 166–174
- 18 Joo JB, Zhang Q, Dahl M, *et al.* Control of the nanoscale crystallinity in mesoporous TiO₂ shells for enhanced photocatalytic activity. *Energy Environ Sci*, 2012, 5: 6321–6327
- 19 Joo JB, Lee I, Dahl M, *et al.* Controllable synthesis of mesoporous TiO₂ hollow shells: toward an efficient photocatalyst. *Adv Funct Mater*, 2013, 23: 4246–4254
- 20 Liu H, Joo JB, Dahl M, *et al.* Crystallinity control of TiO₂ hollow shells through resin-protected calcination for enhanced photocatalytic activity. *Energy Environ Sci*, 2015, 8: 286–296
- 21 Li H, Bian Z, Zhu J, *et al.* Mesoporous titania spheres with tunable chamber structure and enhanced photocatalytic activity. *J Am Chem Soc*, 2007, 129: 8406–8407

- 22 Shi JW, Zong X, Wu X, *et al.* Carbon-doped titania hollow spheres with tunable hierarchical macroporous channels and enhanced visible light-induced photocatalytic activity. *ChemCatChem*, 2012, 4: 488–491
- 23 Wu X, Lu GQM, Wang L. Shell-in-shell TiO₂ hollow spheres synthesized by one-pot hydrothermal method for dye-sensitized solar cell application. *Energy Environ Sci*, 2011, 4: 3565–3572
- 24 Zhao T, Liu Z, Nakata K, *et al.* Multichannel TiO₂ hollow fibers with enhanced photocatalytic activity. *J Mater Chem*, 2010, 20: 5095–5099
- 25 Kondo Y, Yoshikawa H, Awaga K, *et al.* Preparation, photocatalytic activities, and dye-sensitized solar-cell performance of submicron-scale TiO₂ hollow spheres. *Langmuir*, 2008, 24: 547–550
- 26 Yu J, Yu X. Hydrothermal synthesis and photocatalytic activity of zinc oxide hollow spheres. *Environ Sci Technol*, 2008, 42: 4902–4907
- 27 Wang X, Liao M, Zhong Y, *et al.* ZnO hollow spheres with double-yolk egg structure for high-performance photocatalysts and photodetectors. *Adv Mater*, 2012, 24: 3421–3425
- 28 Song X, Gao L. Facile synthesis and hierarchical assembly of hollow nickel oxide architectures bearing enhanced photocatalytic properties. *J Phys Chem C*, 2008, 112: 15299–15305
- 29 Zhu Y, Wang L, Huang G, *et al.* Luminescent and photocatalytic properties of hollow SnO₂ nanospheres. *Mater Sci Eng-B*, 2013, 178: 725–729
- 30 Luo M, Liu Y, Hu J, *et al.* One-pot synthesis of CdS and Ni-doped CdS hollow spheres with enhanced photocatalytic activity and durability. *ACS Appl Mater Interfaces*, 2012, 4: 1813–1821
- 31 Yu J, Yu X, Huang B, *et al.* Hydrothermal synthesis and visible-light photocatalytic activity of novel cage-like ferric oxide hollow spheres. *Cryst Growth Des*, 2009, 9: 1474–1480
- 32 Sun J, Zhang J, Zhang M, *et al.* Bioinspired hollow semiconductor nanospheres as photosynthetic nanoparticles. *Nat Commun*, 2012, 3: 1139
- 33 Born M, Wolf E. Principles of Optics (7th Edition). Cambridge: Cambridge University Press, 1999
- 34 Bohren CF, Huffman DR. Absorption and Scattering of Light by Small Particles. Weinheim: Wiley-VCH, 2004
- 35 Stöber W, Fink A, Bohn E. Controlled growth of monodisperse silica spheres in the micron size range. *J Colloid Interface Sci*, 1968, 26: 62–69
- 36 Zhang Q, Zhang T, Ge J, *et al.* Permeable silica shell through surface-protected etching. *Nano Lett*, 2008, 8: 2867–2871
- 37 Zeng Y, Wang X, Wang H, *et al.* Multi-shelled titania hollow spheres fabricated by a hard template strategy: enhanced photocatalytic activity. *Chem Commun*, 2010, 46: 4312–4314
- 38 Qian J, Liu P, Xiao Y, *et al.* TiO₂-coated multilayered SnO₂ hollow microspheres for dye-sensitized solar cells. *Adv Mater*, 2009, 21: 3663–3667

Acknowledgments Yin Y is grateful for the support from the U.S. Department of Energy, Office of Science, Basic Energy Sciences, Chemical Sciences, Geosciences, & Biosciences (CSGB) Division (DE-SC0002247). Liu H acknowledges the support from the National Natural Science Foundation of China (21501081, 21571089, and 21401091) and the Fundamental Research Funds for the Central Universities (SWU116010 and lzujbky-2015-19).

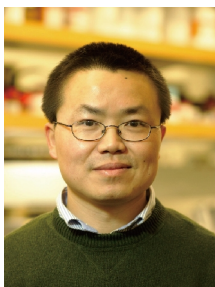
Author contributions Yin Y and Liu H designed the project. Liu H performed the experiments and wrote the paper with support from Yin Y and Joo J. Ma H contributed to the theoretical calculations and analysis. All authors contributed to the general discussion.

Conflict of interest The authors declare that they have no conflict of interest.

Supplementary information Simulations and calculations, high magnification TEM images, XRD patterns, and surface area of the selected TiO₂ hollow shells are available in the online version of the paper.



Hongyan Liu is an associate professor at the College of Chemistry and Chemical Engineering, Southwest University. Her research is focused on the synthesis of nanostructures and their applications in photocatalysis and photoelectrochemical biosensors.



Yadong Yin is a professor at the Department of Chemistry, University of California, Riverside. His research is focused on the synthesis and application of nanostructured materials, self-assembly processes, and colloidal and interface chemistry.

纳米二氧化钛空心球中的多重反射对于光的吸收效率的影响

刘红艳^{1,2,3*}, 马华², Jibong Joo^{2,4}, 殷亚东^{2*}

摘要 本文通过理论模拟和实验相结合的方法,研究了TiO₂纳米空心球内的多重反射和多重散射作用及其对光催化活性的影响.首先通过基于米氏散射理论的模拟,计算了TiO₂空心球的消光、吸收和散射.进而合成了不同尺寸和不同结构的TiO₂.通过对比空心球研磨前后光催化的活性来验证空心球内多重反射是否存在及其对光催化活性的影响.研究指出,TiO₂纳米空心球内部并没有多重反射.空心球之间的多重散射对催化活性的贡献也很小.因此,设计高活性的光催化剂,应该集中在对催化剂晶粒尺寸和晶相的控制,以及引入复合催化剂提高电子空穴的利用效率,而不是材料的几何结构本身.